Visual shape discrimination in goldfish, modelled with the neural circuitry of optic tectum and torus longitudinalis.

David Northmore
Department of Psychological and Brain Sciences
University of Delaware
northmor@udel.edu

Abstract

The ability of fish to discriminate shapes visually is well documented. What is not understood are the neural mechanisms employed by fish and other vertebrates that lack a cerebral cortex to distinguish even simple geometric patterns. All the behavioral and anatomical data in fishes point to the midbrain optic tectum as the essential structure, but physiological studies of it have shown only circular contrast-detecting receptive fields and oriented edge detectors with nothing more elaborate that is reliable. Attempting to solve this conundrum, I built a model of tectum with neuron-like elements. When shown objects moving in space, the model forms an attentional locus that tracks one object on a retinotopic layer of simulated tectal pyramidal neurons. The object's elementary features, when binned together, allow it to be distinguished from other objects to some extent; it fails when objects differ only in the features' spatial relationships, which fish can use for discrimination. The model's solution is to bias the attentional locus to the edges of a shape in imitation of goldfish that naturally attend to the top of shapes. Redirection of the attentional locus from a shape's center is achieved by spatially offsetting synaptic inputs to the pyramidal neurons, effected by the torus longitudinalis (an elongated nucleus at the medial rim of each tectal lobe) and its prolific axonal projections to the pyramidal neurons. The model's shape discrimination was compared to goldfish in the extensive behavioral data of Bowman & Sutherland (1969) who used shapes with points and projections. One test series showed that fish were sensitive to the relative number of points on the tops of shapes. In another, fish could be trained to discriminate points on the sides. By using different offset connections and only one elementary feature detector for small dark spots, the model successfully emulated the two sets of goldfish data, as judged by significant correlations between model response and fish discrimination over 21 pairs of shapes in each series.

Abbreviations: B&S, Bowman & Sutherland (1969); SM, *Stratum marginale*; SO, *stratum opticum*; SFGS, *stratum fibrosum et griseum superficiale*; SGC, *stratum griseum centrale*; SAC, *stratum album centrale*; SPV, *stratum periventriculare*; TL, *torus longitudinalis*; RF, receptive field; RGC, retinal ganglion cell; SSRF, small spot-detecting receptive field; LDRF, large dimming receptive field; IAC, interactive and competitive; GABA, gamma amino butyric acid; mya, million years ago.

Introduction

Up until the time of our review of fish vision (Northmore et al., 1978), goldfish and at least 10 other fish species, had been tested for their ability to discriminate geometric shapes by training, mostly in two-choice operant experiments with food reward. The weight of evidence then showed that discrimination behavior was controlled mainly by features such as points, knobs, or corners, especially at the tops of shapes. Also important, but to a lesser degree, were the orientations of principal contours. Other factors such as size, contrast and color were also influential but are of less concern here. The picture that then emerged was of a visual system that recognized a shape by detecting a limited set of features combined with the features' relative positions on the shape, rather than by constructing a whole-object concept of shapes.

Since then, some fish species have been shown to recognize complex patterns such as the faces of both fish and humans (Parker et al., 2020; Coss & Tyler, 2023; Newport et al., 2016) that would implicate sophisticated discriminative and memory mechanisms. Moreover, goldfish and red-tail splitfins can interpret shape from subjective contours, and in the case of the latter species, recognize a stimulus shape even when partially occluded (amodal completion) (Wyzisk & Neumeyer, 2007; Sovrano & Bisazza, 2009). Fish also seem to experience several classic perceptual illusions (Agrillo et al., 2020). Such capabilities in humans and other mammals are typically ascribed to cortical mechanisms; the fact that fish and other "lower" orders without a cerebral cortex exhibit them might suggest the operation of non-telencephalic or proto-cortical brain mechanisms, that with the emergence of mammals were transferred to the cortex (Zhaoping, 2016). Whatever the merit of that idea, the present modelling study proposes a mechanism for shape discrimination by fishes that is centered in the midbrain and is quite different in operation from the hierarchical, feature detecting mechanisms of cortex (Serre, 2014).

How the discrimination of simple geometric shapes might be accounted for by known neural mechanisms in fishes is a mystery. We can largely rule out a significant role of the telencephalon because its ablation in goldfish does not impair the learning of a circle-square discrimination (Flood, 1975) or other kinds of visual discrimination (Bernstein, 1962; Iwai et al., 1970; Ohnishi, 1991). However, ablation of the midbrain optic tectum eliminates all visual abilities (Yager et al., 1977) except for large-field luminance detection (Northmore & Sharma, 1979). The importance of tectum versus telencephalon is further underlined by the fact that the great majority of optic fibers terminate in tectum, forming a detailed retinotopic map in the superficial layers (Meyer, 1980), whereas only small numbers of optic fibers terminate in the several pretectal nuclei (Robles et al., 2014), which are, therefore, unlikely to contribute much to spatial discriminative abilities. While there are pathways that could transmit visual information from tectum to the telencephalon, they are indirect via relatively small thalamic/pretectal nuclei (Ito & Kishida, 1978; Hagio et al., 2018; Yañez et al., 2018). The few functional studies of teleost pretectum have found visually driven units that responded to spot motion with large receptive fields (Rowe & Beauchamp, 1982; Friedlander, 1983; Wang et al. 2020). Visual units in teleost forebrain respond with habituating and temporally complex spike trains (Saidel et al., 2001). None of these studies indicate anything resembling the shape selectivity of neurons in the ventral stream of the mammalian visual cortex (Serre, 2014).

We must, therefore, look to the optic tectum and its neural mechanisms to understand pattern discrimination in fishes. The tectal layers, *stratum opticum* (SO) and *stratum fibrosum et griseum superficiale* (SFGS), receive most of the retinal ganglion cell terminals whose activity can be recorded with extracellular electrodes and distinguished from postsynaptic cell activity by various criteria. The most comprehensive investigations using these methods in goldfish tectum by the Maximovs and their associates revealed distinct functional types found at characteristic depths in SFGS (Maximova et al. 2019). The units encountered most superficially were directionally selective, responding to edges moved in one of three directions. Next in depth were units sensitive to edge orientation, horizontal or vertical. Also at this depth, but less commonly encountered, were units without sustained activity, sensitive to small spots of positive or negative contrast, but insensitive to large field luminance changes. At a deeper level, there were units with larger receptive fields that responded in sustained fashion to dimming or lightening. The latter two classes are important components in the model proposed here.

The visual properties of tectal neurons in teleosts have been difficult to characterize by electrical recordings and have been a disappointment to seekers of feature detectors. Their responses to visual stimuli are variable, often strongly habituating with repetition, and exhibit large, often multi-center receptive fields (Schellart & Spekreijse, 1976; O'Benar, 1976; Guthrie & Banks, 1978; Sajovic & Levinthal, 1982; Guthrie & Sharma 1991) that seem ill-suited for analyzing the details of shapes.

Advanced techniques of recording and imaging activity in larval zebrafish are providing a wealth of new detail on tectal processing. The data so far that is relevant to shape recognition include demonstrations of selectivity for stimulus orientation (Nikolaou et al., 2012) and size. Small and large stimuli differentially activate populations of superficial inhibitory neurons (SINs) with somas at the tectal surface and neurites at various depths in the retinorecipient neuropil (SO & SFGS) that engage with periventricular neurons, possibly sharpening their size-selectivity (Del Bene et al., 2010; Preuss et al., 2014).

Despite these advances, we still have no evidence that tectal neurons elaborate shape analyzers. A 60-year absence of such evidence is beginning to look like evidence of absence. Evidently the discriminative functions of tectum are achieved in a radically different fashion from mammalian visual cortex. Instead of the multiple retinotopic maps arrayed in separate cortical areas, connected quasi hierarchically (Felleman & Van Essen, 1991), tectum possesses a single retinotopic map composed of several substrata receiving input from different kinds of retinal ganglion cells (Robles et al., 2013). Because most tectal neurons processing this input extend radially through the tectum, it is hard to see how a hierarchical network of any depth could be formed, an architecture considered key to mammalian pattern vision. Understanding that, it is claimed, has been advanced by modelling vision with deep learning in hierarchical convolutional neural networks (Mély & Serre, 2017). While the recognition abilities of these systems are impressive, they differ from brains in their learning algorithms, their exclusively feedforward architecture and, most notably, their inability to attend selectively.

Attention in tectum

It can be argued that the evolution of vision for catching prey immediately necessitated the invention of selective attention. The first jawed fishes (ca. 500 mya) that pursued other mobile animals needed to hold a focus of attention on one of them in order to direct an effective attack. Prey seeking must also have required the development of discriminatory abilities ensuring pursuit of edible species rather than the distasteful or the dangerous. The ability to form an attentional focus for preferentially analyzing a region of the visual field and to allow the focus to track a moving object could then have given rise to a form of object perception in which the constituent features of the object are bound (Triesman & Gelade, 1980; Reichenthal at al., 2020), allowing it to be classified into useful categories such as edible, inedible, noxious, inanimate etc. The requirements for a mechanism to do this can be stated quite simply: (i) a retinotopic representation of the scene by simple analyzers, such as for size, edge orientation and color, (ii) a winner-take-all type of attention-forming focus in retinotopic coordinates, (iii) selection of those features present in the focus, and (iv) classification based on those selected features leading to approach or avoidance behavior.

The idea for a plausible neural implementation of this mechanism comes from a modelling study (Northmore, 2017) that demonstrated how midbrain mechanisms, specifically in the tectum and *torus longitudinalis* (TL) could enable a predator fish to hold a focus of attention on the prey it is chasing despite rapid displacements of the retinal image during saccadic eye movements. The model proposes that the attention-focusing mechanism involves a "pointer network" composed of a numerous cell type in tectum, the pyramidal neuron with soma in SFGS (Type I of Meek & Schellart, 1978) (See Figs. 6 & 7). It receives input from retinal terminals in SO and SFGS and has an extensive dendritic tree in the most superficial tectal layer, the *stratum marginale* (SM). There, it receives excitatory input from the marginal fibers originating in granule cells of the TL, a paired, elongated nucleus attached to the medial edges of the tectal lobes (Vanegas et al., 1979; Wullimann, 1994; Folgueira et al., 2007). The model assumes that pyramidal cells are mutually inhibited via interneurons to make a winner-take-all configuration. One visual stimulus object, the most salient out of many that may be present in the visual field, will then activate a cluster of pyramidal neurons at its retinotopically corresponding position in tectum, forming the attentional focus. Given some additional neural circuit refinements, the focus is able to track the object moving in space. However, an eye saccade shifts the retinal image of the object too rapidly for it to be tracked, and the focus of attention will likely settle on a different target object. Nevertheless, tracking can be immediately restored by "predictive priming" of pyramidal cells at the place in tectum that represents the object after the saccade. This is achieved by TL transmitting two signals through SM to the pyramidal cell dendrites: (i) the pre-saccade position of the attentional focus and (ii) a corollary discharge giving saccade direction and amplitude. Only those pyramidal dendrites that bear the appropriate synapses decode the TL signals and prime the neuron by depolarizing it. The attentional locus now becomes established at the new tectal position and tracking resumes.

For the modelling of shape discrimination investigated here, the focus of attention, formed by heightened activity in a cluster of neighboring pyramidal neurons is supposed to select stimulus features that are close together in the retinal image, thereby "binding" them as a potential object. The focus of attention could then enable only the neural elements responding to those stimulus

features, wherever the object is in the visual field. To obtain a reading of the object's qualities, it is only necessary to collect or "bin" all the activity of the attentionally-enabled feature units across the tectal lobe. The resulting binned components provide a vector for identifying the object. The principle can be implemented with known tectal circuitry, while providing an explanation for how the basic visual feature information present in the superficial tectum could be used. However, this mechanism is unable to distinguish two objects with the same feature content but different spatial relationships between them, something that fish can clearly do (Sutherland & Bowman, 1969).

An aim of this paper is to show with the help of modelling, how neural structures in the midbrain of fishes could implement shape discrimination along these lines while improving on the simple binning mechanism. The most extensive studies of goldfish shape discrimination have been those of Stuart Sutherland and his associates undertaken in the development of his theory of pattern discrimination in animals and humans (Sutherland, 1968). Some of the data they generated by training goldfish on stimulus pairs and performing transfer tests to uncover the features used for discrimination will provide tests of the model.

Methods

In the Bowman & Sutherland (1969) experiments ("B&S" henceforward) the training and testing of goldfish used shapes cut from ¼" black plastic on a white background, each shape being separated horizontally by 5" (12.7 cm) and held at its center a small trough for a food pellet or a similar-looking inedible pebble. Each trial began with the fish swimming through an opening 12" (30.5 cms) from the shapes and swimming up to one of the shapes to receive either the food reward or the pebble, depending on the contingencies of the experiment. The decision point was not defined in these experiments but could have been between 30.5 and 6.5 cm, the latter distance set by the depth of a dividing screen projecting from the plane of the shapes.

The discriminations with the simulated neural system used 45 of the B&S stimulus shapes. They were scaled in size to present roughly the same area as the B&S stimuli (14.4 cm^2). During a simulation run each shape was individually moved towards the camera from a starting distance of 19 cm up to 7.5 cm, representing changes in visual angle from about 11.4 to 28.1 degrees, or a width increase by a factor of 2.46. The rate of approach was 0.3 pixels/tick over 200 ticks. The starting positions of stimuli were randomized from trial to trial within a 32 x 24-pixel rectangle so that they activated different successions of pixels and receptive fields, leading to substantial trial-trial response variability.

The Network

The methods for network construction and simulation are essentially those described for a model of tectum and TL (Northmore, 2017). A custom simulation program written in Borland Delphi Pascal allowed layers of artificial neural units to be arrayed in two dimensions of "brain space" and provided various methods for interconnecting them. Figure 2 shows the layers of the current network, the activity within each layer at a moment in time and the connections of a single representative unit in each of them. Typically, each unit of a source layer projected multiple synapses centered on the topographically corresponding point in the destination layer, with the synaptic weights falling off from the center of projection according to a radial Gaussian function.

A connection was specified by its maximum weight and was either excitatory or inhibitory, indicated by the green and red squares respectively in Fig. 2. Layers were composed of linear threshold units or of IAC units, the latter having been employed in Interactive and Competitive networks (McClelland & Rumelhart, 1988. See Northmore, 2017 and its supplemental data for details). The feature of IAC units is that they obey 1st-order dynamics, in this case with a decay time constant of 10 simulation ticks. Consequently, an IAC unit in this network settles over time at a level of activation determined by the various excitatory and inhibitory inputs impinging upon it.

The simulation program used GLscene, a 3-D graphics package based on OpenGL to present the black shape stimuli as sprites moving in 3D space against a gray background. The GLscene camera, representing the goldfish eye, viewed a rectangular 120 x 160-pixel array that was sampled by two kinds of difference-of-Gaussian receptive fields (RFs) emulating retinal ganglion cells (RGCs), and these constituted the visual input to the model. The smaller type, the small spot-detecting RF (SSRF) was designed to respond in a sustained fashion to the points and projections on the outlines of the black test shapes. It was composed of a central OFF Gaussian of 1.6 degrees half-maximum diameter with a Gaussian ON surround of half-maximum diameter of 5.6 degs (see Fig. 7). The visual field was sampled by a 35 x 25 rectangular array of such units. The other field type, the large dimming RF (LDRF) was designed to give a sustained response to darkening within its receptive field with a half-maximum width of 15 degs but with no antagonistic surround (see Fig. 6). The visual field was sampled by a 17 x 12 rectangular array of such units.

In the previous simulation study (Northmore 2017), the layer of central importance was the "pointer network" whose activity formed an attentional focus for selecting incoming sensory information. It was identified with the population of pyramidal neurons in fish tectum. Here, the corresponding layer, composed of IAC units, is called the ObjLoc layer as it locates or points to the current object of interest in the visual field (see Fig. 2). To implement the ObjLoc layer, each of its units should receive excitatory topographic visual input while making local connections that (i) inhibit other units in the ObjLoc layer, thereby forming a winner-take-all circuit and (ii) excite units locally in the ObjLoc layer to allow the locus to move smoothly with movement of the attended object. The other layer type required for an attentional network are the "Pool" layers, also composed of IAC units and each subject to local inhibitory feedback. These layers would receive and process a visual submodality (e.g. color, orientation, size) and interact with the ObjLoc layer, in a bidirectional fashion. In the current network, ObjLoc's focus is activated from only one such pool (LPool), that indicates the center of dark shapes. ObjLoc's focus enables the corresponding place in another pool (SPool) that responds to the pointed features of stimulus shapes. The model's output is the activity of SPool under the focus of ObjLoc. Details of these layers and their connections follow.

In the network shown in Fig. 2, the visual field is sampled by the LDRFs and the SSRFs. Each LDRF connects excitatorily with Gaussian spread to LPool. Each LPool unit connects firstly, to excite a corresponding linear threshold unit in a layer of inhibitories (Linh) that connects back to

Excitatory connections to ObjLoc	B&S shape Group	Goldfish – Model correlation	Significance 2-tailed t-test, 19 d.f.
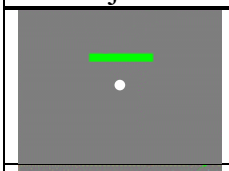	I	0.596	$t = 3.233 \quad p < 0.01$ **
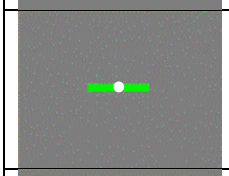	I	-0.398	$t = -1.892 \quad p > 0.05$
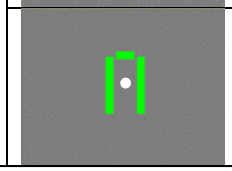	III	0.481	$t = 2.393 \quad p < 0.05$ *

Table 1. Three mappings of connections to ObjLoc from a single unit in LPool (left column, white disc). Each green bar represents a row or column of equally-weighted excitatory synapses onto the ObjLoc layer. The first row of the table shows a control condition without vertical offset that gave no significant correlation between goldfish transference and model response on Group I test pairs; the second with a vertical offset gave a significant positive correlation on Group I; the third with vertical and lateral offsets gave a significant correlation on Group III test pairs.

it inhibitorily, and secondly, to inhibit all other LPool units. Both of these connections limit the gain of this dimming pathway, focusing its activity pattern to what is roughly the center of gravity of a stimulus shape. Thirdly, each LPool unit projects excitatorily to the ObjLoc layer in a spatial pattern to bias the attentional focus in various ways. Three such patterns used are illustrated in Table 1.

Upward biasing of attention was achieved by the 1st row pattern in Table 1. A unit in LPool, exemplified by the white disc, makes excitatory connections (green) to a horizontal row (length = 9) of ObjLoc units, 3 rows above. The effect is shown in Fig. 1 where an M-shape is advanced toward the viewer and simultaneously shifted rightward. The LPool activity centroid tracks near the center of the stimulus shape while the ObjLoc activity centroid floats above. The LPool centroid rises a little above the center because it is in a positive feedback loop with ObjLoc via Linh. There is also some divergence of the two tracks as the image expands keeping the attentional focus hovering near the top.

Figure 1. The M-shaped figure was moved rightward and toward the camera. The position of the centroid of LPool is shown in red; that of ObjLoc in orange.

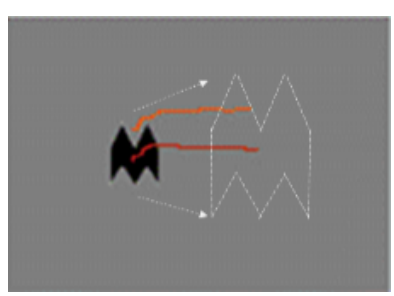

The sharp points of shapes are responded to by the SSRFs. As Fig. 2 shows, SSRFs inhibit their topographically corresponding linear threshold units in the layer Sinh, which in turn topographically inhibit units in SPool. Because the entire Sinh layer is biased on (orange = +ve activation) SPool is generally inhibited (blue = -ve activation), and any points of the stimulus shape leading to SSRF activation will disinhibit topographically corresponding units in SPool. However, the inhibition of SPool is too strong to allow the stimulus-dependent disinhibition alone to activate its units, but SPool units can be activated if they are also subject to excitatory drive from ObjLoc. Since this comes from a band of excitation (orange in ObjLoc) that hovers at the top of the shape, the SPool activation in total will depend on the number of points at the top. The final output of the network to the shape being analyzed is the summed response of SPool.

Although the goldfish performing these visual discriminations would most probably use the front of its visual field, involving both eyes and both tectal lobes, I am making the simplifying assumption that each test shape is processed one at a time by one tectal lobe with a spatially uniform input from RGCs of the opposite eye (Schwassmann & Kruger, 1965).

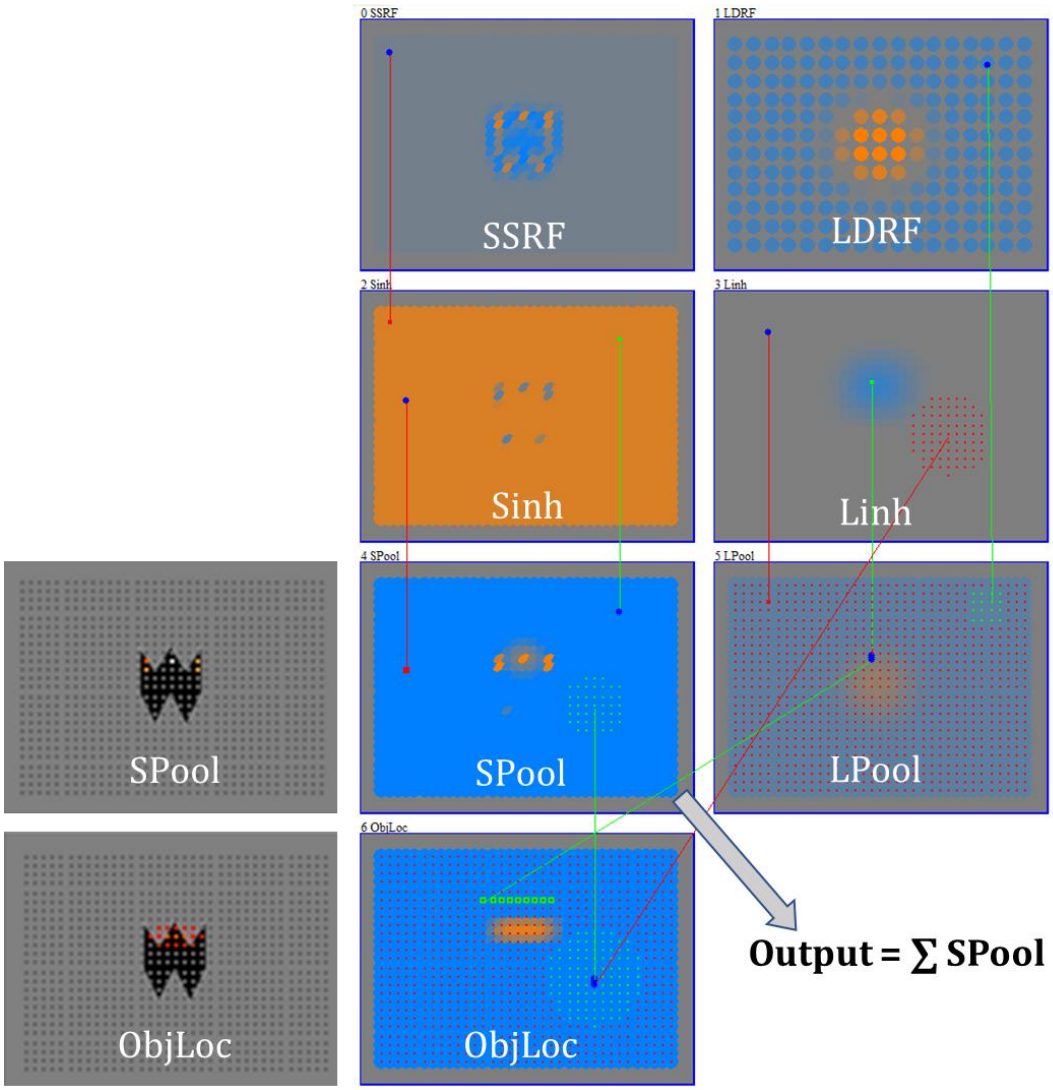

Figure 2. The network in action. The two rightmost columns show the layers currently processing the W shape during its approach. Orange is positive unit activation; blue is negative unit activation. Each small dark blue disc shows a single, arbitrarily selected source unit in its layer; the line from it, its connections. Green: excitatory connections and synapses; Red: inhibitory connections and synapses. Leftmost column: the W shape overlaid by unit activity; Upper: colored dots show SPool units responding to points on top; Lower: ObjLoc responses enabling SPool. Output of the model is the summation of all SPool unit responses.

Results

To emulate the shape transfer experiments of B&S, each of the 45 individual black on gray shapes was input to the network by placing it randomly within a central rectangle (32 x 24 pixels) and looming it toward the camera over the course of 200 simulation ticks, equivalent to a 2-sec approach time. Time was not a critical factor in the simulation as the decay time constants of the IAC units were short in comparison to the simulation period. The looming of each stimulus was repeated 20 times, generating waveforms for the summed responses of SPool such as those shown in Fig. 3 **B**. The randomization of the stimulus starting positions and their subsequent trajectories introduced trial-to-trial variation in the network response as the receptive fields and network connections were activated differently on each trial. Varying stimulus position in this way was important for demonstrating position invariance of the model's discrimination abilities claimed here.

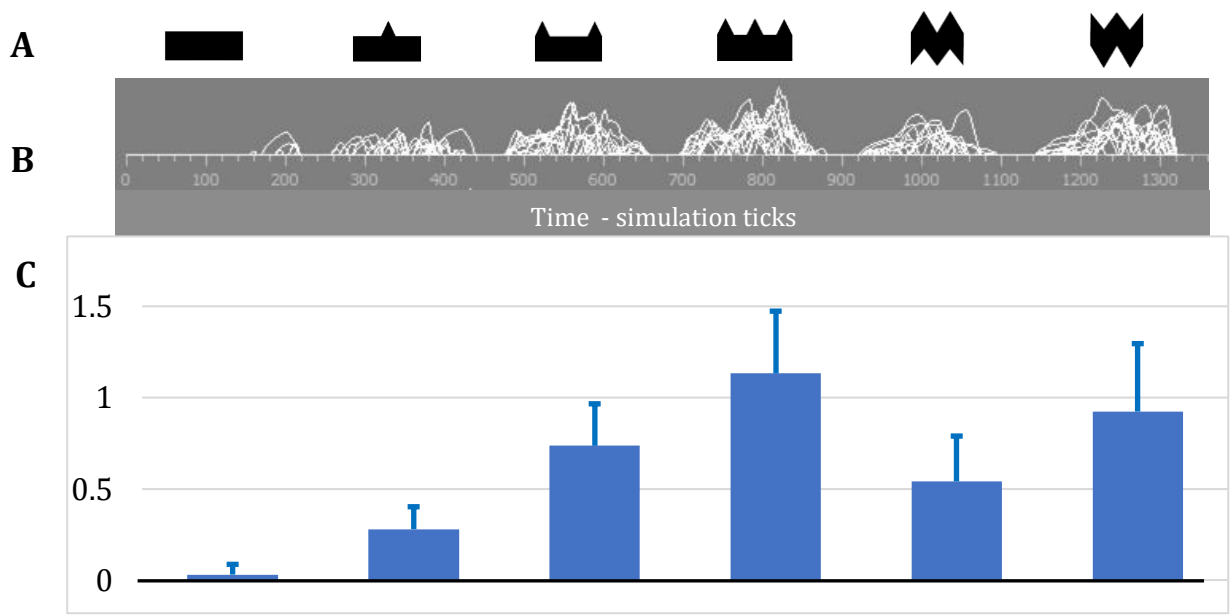

Figure 3. Network responses derived from the summation of all SPool unit responses to six shapes (**A**) accumulated over 20 approaches (**B**). **C** shows the average of the 20 responses integrated over time, with their standard deviation.

Network responses to the individual shapes were obtained by averaging all the SPool unit responses over 20 approaches (see Fig. 3 for examples). The model's discrimination of a pair of shapes, one designated positive by B&S, the other negative, was assessed by subtracting the averaged SPool response to the negative shape from that to the positive shape, the difference giving the Model Response in figures 4 and 5. This value was compared with the corresponding goldfish "Transference" value for the stimulus pair using B&S's percent correct (P), adjusted for 50% correct responding by chance i.e. (P-50)/50 (Abbott's formula). Transference, so defined, varied from about 0 to 1.0 making it comparable to the range of Model Responses, both of which are plotted in figures 4 and 5.

Upward biasing for Group I

In B&S's Group I test, fish were trained to discriminate from (leftmost pair in Fig 4), giving the fish the opportunity to use 2 vs.1 points on top, and/or 3 vs 2 points on the bottom. Figure 4 presents the goldfish data (orange) for the other 20 pairs showing that transference was highest when there was a preponderance of points on top of the positive shape (upper in each pair). B&S concluded that transfer was governed by the relative numbers of points on top, not the absolute number.

This tendency of goldfish to attend to the uppermost discontinuities of shape outlines requires a means of locating the tops. To summarize the method employed by the network of Fig 2: locate the center of darkness in the shape using an array of large OFF receptive fields and send its position to ObjLoc with an upward offset (Table 1, 1st row).

Figure 4 presents the model response (blue) for all 21 pairs in the B&S Group I test. Many of the high and low points of the goldfish performance are paralleled by the model response. Thus, 'positive' shapes with more points on top than their negative counterparts yielded high responses, whereas those with few or no points on top yielded the lowest responses. The greatest discrepancies, where the model responded excessively, were for positive shapes with pronounced vertical projections like the crosses (tests 10, 11) and shapes with a preponderance of upward

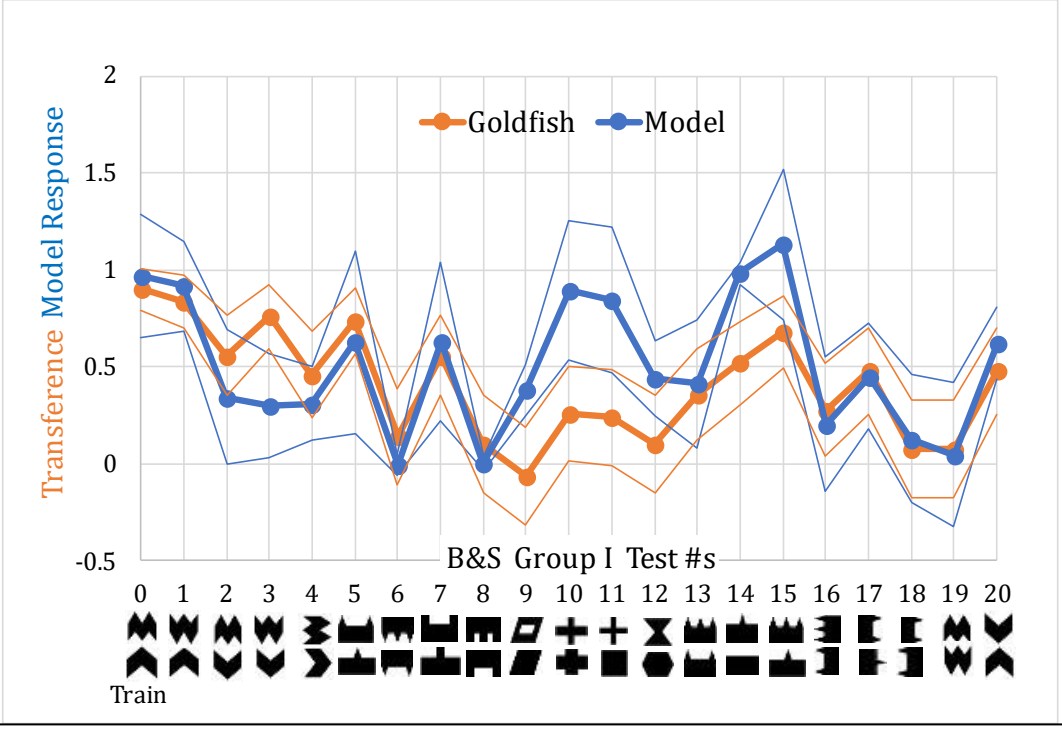

Figure 4. Bowman & Sutherland's Group I goldfish behavioral transference (orange) compared to the model response (blue). Fish were trained to 95% correct on the leftmost test pair and tested on the other 19 pairs. The goldfish data and 95% confidence intervals from the binomial distribution based on 60 trials were corrected for 50% chance responding by Abbott's formula. The model data points and 95% confidence intervals were based on 20 trials each.

projections (14, 15). A significant correlation (r=0.596) between goldfish transference and model response was obtained (Table 1, 1st row). To show that the vertical offset was critical to the model's emulation, a control condition with no offset was run, yielding no significant correlation (Table 1, 2nd row).

Left, right and upward biasing for Group III

In the Group I experiment of B&S, transference to shapes with points on the sides was poor, in keeping with the goldfish's natural tendency to focus attention on the tops of figures. In their Group III experiment, fish were trained on the pair of shapes and with points on both left and right sides in the ratios 3:2 and 2:1 (Fig. 5 leftmost pair). Fish successfully achieved criterion discrimination (95%) and were tested on the pairs shown in Fig. 5. They showed good transfer to the "pointier" shape pairs (1-3 and 5-8) whether the points were on the left or right, but little or no transfer to "pointless" shapes (9-12), nor to pairs of mirror-image "pointy" shapes (19, 20). They transferred well to pair 4 that differed in the number of points on top, presumably reflecting their natural preference.

To show that the model can also emulate these data, the connections from each LPool unit to ObjLoc were made to be columns of excitatory synapses 10 units high biased 3 units leftward and rightward, and a row of synapses 3 units long and biased upward by 5 units to form the pattern shown in Table 1, 3rd row. Each individual shape of Fig. 5 was loomed to the camera to collect the integrated responses of SPool units as before. The integrated responses to the positive

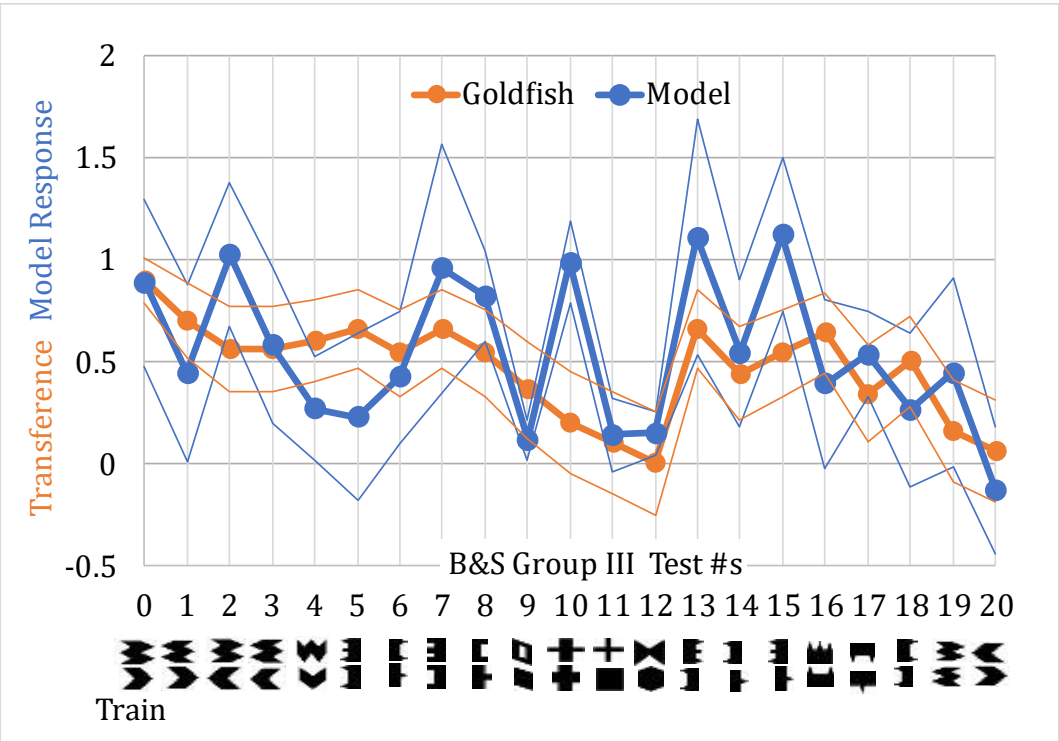

Figure 5. B&S's Group III goldfish behavioral transference (orange) compared to the model response (blue). Details as for Fig. 4.

and negative shapes of each test pair were differenced to give the Model Response, which was plotted with the goldfish Transference in Fig. 5.

The model generally reproduced the overall profile of the goldfish transference, albeit in more exaggerated form, yielding a significant correlation of 0.481 (Table 1, 3rd row). The only significant discrepancy was the high response of the model to the two-crosses pair (#10); the thin cross bars projecting from a thick body strongly activated the point detectors, more so than they did when projecting from a thin body (#11). The reason is that the overall black area of the latter cross was relatively small, leading to a weaker drive of LPool to ObjLoc and weaker point detection. Eliminating test #10 gave a higher correlation ($r = 0.593$, $p < 0.01$).

Discussion

B&S concluded that the main determinant of goldfish discrimination performance was the relative number of points at the tops of shapes (see also Sutherland & Bowman, 1969), rather than the absolute numbers of points on the training shapes. The model similarly responds to relative numbers because of its simple decision rule: treat the shape with the higher SPool activation as the positive stimulus. The model, applying this rule, also accounted for goldfish behavior when biased to attend to left, right and top edges of shapes.

Neural implementation

Here I attempt to link the structure and connectivity of the network with the neurology of the visual system in fishes.

The two receptive field types, SSRF and LDRF, providing visual input to the model, have their counterparts among goldfish retinal ganglion cells. LDRF is a sustained OFF receptive field without antagonistic surround subtending 15 degrees. These resemble alpha-like retinal ganglion cells in goldfish (Cook et al., 1992), that exhibit sustained OFF-firing and subtend 13-24 degs under light adapted conditions (Northmore & Oh, 1998). SSRF, the OFF-center ON-surround receptive field had an overall half-width of 5.6 degs, close to the smallest RGCs of goldfish (Northmore, 1977). Its spatial frequency response peaked at 0.33 cycles/degree, which is also where the behavioral contrast sensitivity function of goldfish peaks (Northmore & Dvorak, 1979), corresponding to a point-spread function with a center subtending 1.6-1.7 degrees, which matches the OFF center half-width of SSRF.

Both electrical recordings and Ca^{++} imaging from superficial tectum show further processing of retinal inputs, elaborating specificity for size, orientation, direction of motion and color (Gabriel et al. 2012; Maxsimova et al. 2019; Nikolaou et al., 2012; Nilo et al., 2021). These provide the ingredients for the binning method of object recognition, whereby the object being attended is specified by the amounts of the different features present within the current focus of attention. However, the simulation results suggest that recognition of black shapes can be largely accounted for with only one type of feature detector, the SSRFs, that are selective for small dark points.

LDRFs in a relatively coarse array, connect excitatorily and topographically to LPool, a layer of units that can be identified with the Type X neurons of Meek & Schellart (1978), also known as

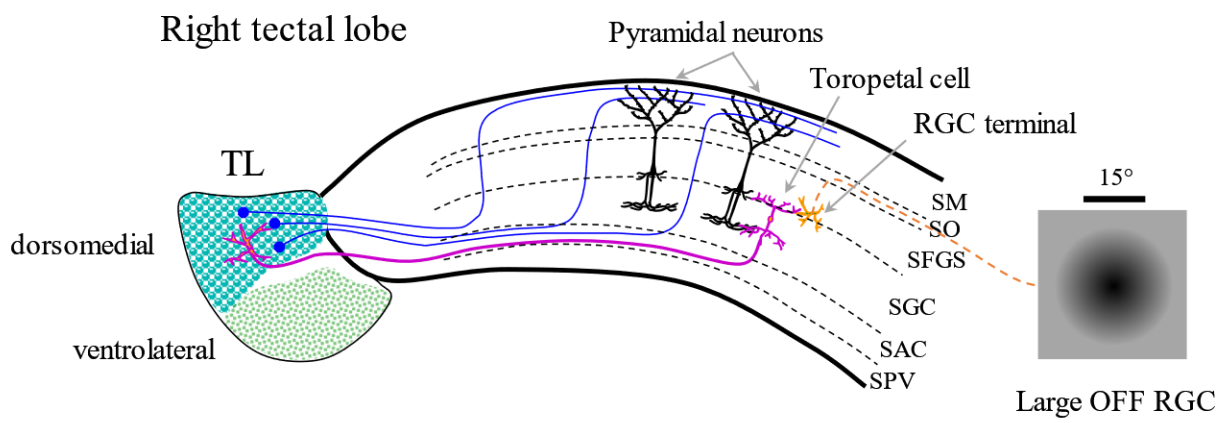

Figure 6. Schematic of retino-tectal-TL circuitry. Retinal ganglion cells with large OFF receptive fields terminate in deep SFGS, synapsing excitatorily with Type X toropetal neurons which innervate dorsomedial TL. TL granule cells send marginal fibers through SM, synapsing excitatorily with the apical dendritic trees of Type I pyramidal cells. Depending on how toropetal inputs are switched in TL, different offsets in the priming of pyramidal cells can be achieved. This figure shows how RGC activation can lead to pyramidal cell priming at a higher position in the visual field.

toropetal neurons because they project to dorsomedial TL (Xue et al., 2003; Folgueira et al., 2007) and are responsible for TL's retinotopic dimming activity (Northmore, 1984; Robles et al., 2021). The dendrites of toropetal neurons in goldfish ramify in deep SFGS and mid *stratum griseum centrale* (SGC), which is where the axons of dimming RGCs terminate (Robles et al., 2021) (see Fig. 6). It is also noteworthy that the toropetals ramify at the same depth as (i) the pyramidal neurons' soma and near-soma dendrites and (ii) the deep axonal and dendritic ramifications of pyramidal neurons (Xue et a. 2003; Folgueira et al. 2020). The close relationship between these two neuron types suggests exchanges of information can take place between them such as were previously postulated by Northmore (2017) as part of the mechanism to maintain attention across saccadic eye movements. In the present network, the connections of special interest, those from the toropetals (LPool) to the pyramidal neurons (ObjLoc) are the excitatory, displaced connections (Table 1; Fig. 2). The key idea here is that the displacement is achieved at the final arrow in the pathway: toropetal → dorsomedial TL → marginal fibers → pyramidal neuron dendrites (see Fig. 6). The position of the center of the stimulus shape is represented by an activity peak on the layer of toropetals (LPool) and is sharpened by local and lateral feedback inhibitory connections between Linh and LPool. The toropetals, where their activity peaks, excite neurons in dorsomedial TL at the topographically corresponding position along TL's length. There, TL neurons transmit excitation through SM in a set of fibers that preferentially synapse with the dendrites of pyramidal neurons at a more dorso-medial position in tectum than the peak of activity in the toropetal layer, i.e. corresponding to a higher position in the visual field. This is shown in Fig, 6 by a second, more medially situated pyramidal neuron.

According to the model, the neural circuitry determining the center of a shape is driven by a dimming pathway. It is interesting to note that Mackintosh & Sutherland (1963) reported that black on white shapes were much easier for goldfish to learn than white on black, evidence of a

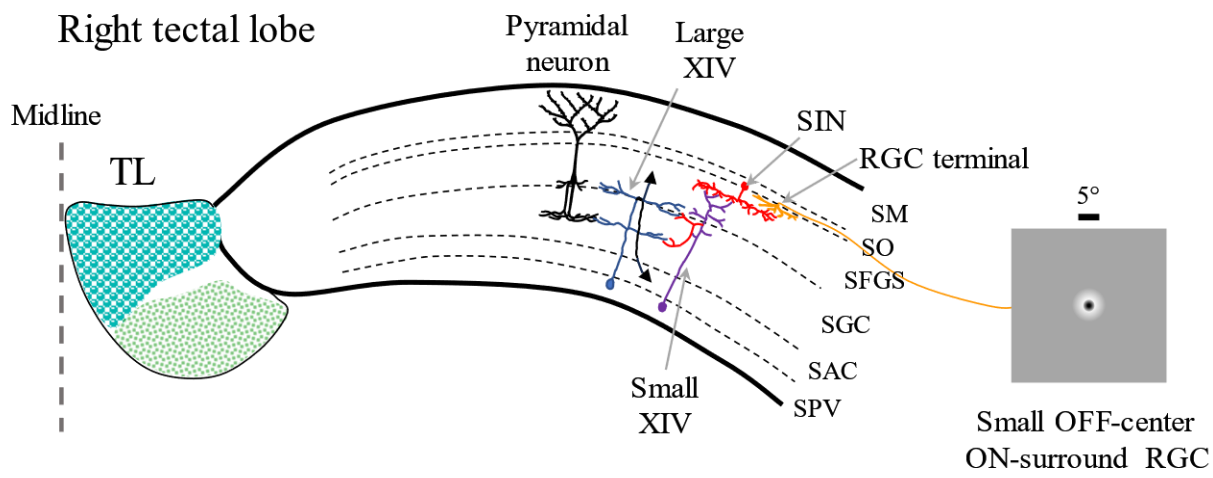

Figure 7. Schematic of tectal circuitry. Retinal ganglion cells with small OFF-center, ON-surround receptive fields terminate in superficial SFGS, synapsing excitatorily with superficial inhibitory neurons (SIN) that inhibit Small Type XIV neurons; their axons inhibit neighboring Large Type XIV neurons which are excited by the axonal arbors of pyramidal cells. The output of the system is transmitted by the Large Type XIV axons, both ascending and descending (black arrows). Inhibitory processes shown in red.

special role of dimming pathways whose characteristics and origins have been discussed elsewhere (Northmore, 2023).

The identification of the neural basis in fish tectum for the point-detecting circuitry can only be tentative at this stage but a possible scheme for implementing the network is shown in Fig. 7. The small OFF-center, ON-surround RGCs form terminal arbors in a superficial sublayer of SFGS. The sign reversal of the retinal input on to the inhibitory Sinh layer could be performed if the retinal terminals were to excite the superficial inhibitory interneurons (SINs) that ramify in these superficial layers (Preuss et al., 2014) which in turn would inhibit the neurons corresponding to Sinh layer. A putative assignment of Sinh units would be to the small Type XIV neurons of Meek & Schellart (1978) which have short processes at different depths in SFGS and SGC. If these are equivalent to the non-stratified periventricular neurons of zebrafish larvae (Robles et al., 2011), their branches in SFGS would be dendrites, contacted and inhibited by the SINs; while their axons would be GABAergic, inhibiting the neurons composing the SPool layer. Appropriately, the small Type XIV neurons in goldfish were shown by Guthrie & Sharma (1991) to be tonically active, providing the background inhibition for SPool, and they were also modulated by visual stimulation. SPool neurons are proposed to be large Type XIV neurons whose dendrites ramify at the border of SFGS and SGC, and in the middle of SGC. Either or both of these dendrites could be the targets of inhibition from the small Type XIV. The deeper branches in mid SGC are positioned to receive drive from the pyramidal cells, thought to be cholinergic (DeMarco et al., 2020). These large Type XIV also have axons, usually branching into two, one of which exits tectum (Kinoshita et al., 2006).

Next, the model requires a means to collect activity from the feature pools across both lobes of tectum for deciding which shape to approach. There should also be separate short-term memory

storage of feature activation pertaining to each of the stimulus shapes over the few seconds it takes the fish to make its choice, accumulating information about the two disriminanda until one wins out. These processes, while possibly involving extra-tectal centers, are likely anchored to the retinotectal map because they drive approach behavior to the chosen shape, and even to the edges of the shape that decide the discrimination, because as B&S observed, goldfish snapped at the tops or at the sides of the stimulus shapes, depending on their training. The pathways from tectum to premotor centers in the brainstem reticular formation controlling approach can be understood as a set of labelled lines from different tectal regions commanding turning movements of appropriate amplitude (Helmbrecht et al., 2018).

What is being learned?

Sutherland's (1968) theory held that learning a pattern discrimination first involves learning to "switch in" stimulus analyzers that are suitably discriminative for the task, and then learn to associate those analyzers with an appropriate behavioral response, such as approach or avoid. The present model has some bearing on the first stage. I chose what seemed to be a successful type of analyzer for discriminating the B&S shapes, namely the SSRFs, but in reality, a number of basic analyzers for size and orientation are available from neuronal elements in superficial tectum. To use these for discrimination is simple in principle. Instead of accumulating activity in SPool only, accumulations in pools for different line orientations and stimulus sizes would effectively generate a feature vector for the attentionally selected stimulus object. If approach to this object leads to reward, a Hebbian-type pattern associator could adjust the weight of each vector component to raise approach probability on a later trial. Thusly, appropriate analyzers are "switched in."

The mechanism just sketched, in effect, throws all of an attended object's features into one bin; features of a different object, attended to later, will go into another bin, allowing the two to be discriminated. This process would have been immediately available to primitive creatures with the kind of basic, winner-take-all visual attention modelled here. An obvious limitation to the bin principle is that the feature accumulation takes place without regard to the spatial relationships between features.

TL as an attentional lens

The ray-fined fishes, the actinopterygians, when they emerged some 400 mya developed a tectal add-on, the TL (Yamamoto & Hagio, 2021), which I maintain allows visual attention to be deflected in a controlled fashion. The predictive priming model for holding attention on a prey object in the face of eye saccades is an example (Northmore, 2017). That model envisioned TL converging two kinds of information onto the tectal pyramidal neurons: the pre-saccade position of the object, and the upcoming saccade vector. The two together could be decoded by a learned pattern of synapses on pyramidal neuron dendritic trees leading to the priming of pyramidal neurons laterally displaced to the post-saccade position. Combining the spread of pyramidal dendrites and the spread of a TL neuron's axons across tectum, which may be considerable (DeMarco et al., 2021), the system could perform shifts of up to 30 degs of visual angle, the maximum amplitude of goldfish saccades.

The current model also envisions displacements of the focus of attention, in this case for selecting features from parts of an object. Binning these allows discriminations between many more patterns. The B&S experiments and the emulation of them have shown that fish can displace attention not only upwards, as they seem to do naturally, but also to both sides, and to do so simultaneously, representing a diffusion of attention. If the predictive priming theory is any guide, displacements and diffusions of up to 30 degs may be possible, allowing a good measure of constancy in the assessment of features of retinal images of different sizes. Thus, TL seems to be an adjustable refractor of the spotlight of attention.

To achieve control over TL's refractions, one might assume an arrangement analogous to saccadic predictive priming (Northmore, 2017) in which TL transmits two kinds of signals to specify attentional shifts. As in that model, the attended object's center is represented by a patch of salient retinal activity, in this case relayed via the toropetals to TL, whose granule cells distribute activity through SM over a wide swathe of tectum centered on the object's representation. Instead of a saccadic corollary discharge in TL, a task-related control signal is generated along the length of TL specifying the direction and extent of deflection of the focus from the object's center. As in the saccadic model, the extensive pyramidal dendritic trees with a learned pattern of toro-pyramidal synapses decode the two types of signals emanating from TL, leading to the activation of the appropriately shifted pyramidal neurons. The source of the control signals in TL can be surmised to descend from the telencephalon via pretectal nuclei (Wulliman, 1994; Yañez et al., 2018; Xue et al., 2003; Folgueira et al., 2020; Yamamoto & Hagio, 2021). Learning a discrimination, therefore, not only requires switching in the right feature analyzers, but also controlling TL to make attentional refractions for the task at hand.

Implications for theories of pattern recognition

It is interesting to consider how the present modelling effort bears upon Sutherland's (1968) theory of pattern recognition, in particular, whether it has solved any of the 12 conditions that he stipulated for a satisfactory theory. Half of his conditions have been satisfied successfully by the model, the remainder being beyond its scope. His *Position Invariance* is well handled and *Size Invariance*, up to an extent determined by TL's spread of priming capacity. *Brightness Invariance*, or more precisely contrast-reversal invariance, could be handled with receptive fields of reverse contrast preferences. *Lack of Invariance under most Rotations* and *Confusions Made between Patterns*, in certain instances, could both be explained by arrangements of TL bias, for example to tops but not to sides. Lastly, his *Consistency with Physiological Knowledge* has been the watchword of this study.

The thrust of Sutherland's theory was that the output of the feature processors leads to the writing of descriptive rules for shapes in a store during learning, and that the outcomes of subsequent testing depend on how these outputs match the descriptions. What neurally inspired modelling has shown here, as in other instances, is how rules can, and should be superseded by networks (Rumelhart & McClelland, 1986).

References

Agrillo, C., Santacà, M.., Pecunioso. A. & Petrazzini, M.E.M. (2020) Everything is subjective under water surface, too: visual illusions in fish. Animal Cognition 23:251–264. https://doi.org/10.1007/s10071-019-01341-7

Bernstein, J.J. (1962) Role of the telencephalon in color vision of fish. Experimental Neurology: 6, 173-185. https://doi.org/10.1016/0014-4886(62)90001-8.

Bowman, R. & Sutherland, N.S. (1969). Discrimination of 'W' and "V" shapes by goldfish. Quarterly Journal of Experimental Psychology 21: 69-76. https://doi.org/10.1080/14640746908400198

Cook, J. E., Becker, D. L. & Kapila, R. (1992). Independent mosaics of large inner- and outer-stratified ganglion cells in the goldfish retina. The Journal of Comparative Neurology 318: 355-366. https://doi.org/10.1002/cne.903180402

Coss, R.G. & Tyler, C.L. (2023) African jewel fish (*Hemichromis bimaculatus*) distinguish individual faces based on their unique iridophore patterns. Animal Cognition. https://doi.org/10.1007/s10071-023-01790-1

Del Bene, F., Wyart, C., Robles, E., Tran, A., Looger, L., Scott, E.K., Isacoff, E.Y., Baier, H. (2010). Filtering of visual information in the tectum by an identified neural circuit. Science 330: 669-673. https://doi.org/10.1126/science.1192949

DeMarco, E., Tesmer, A.L., Hech, B., Kawakami, K. and Robles, E. (2021). Pyramidal neurons of the zebrafish tectum receive highly convergent input from torus longitudinalis. Frontiers in Neuroanatomy. 15:636683. https://doi.org/10.3389/fnana.2021.636683

DeMarco, E., Xu,, N., Baier, H. & Robles, E. (2020) Neuron types in the zebrafish optic tectum labeled by an id2b transgene. The Journal of Comparative Neurology 528:1173–1188. https://doi.org/10.1002/cne.24815

Felleman DJ & Van Essen DC (1991) Distributed hierarchical processing in the primate cerebral cortex. Cereb Cortex 1:1–47. https://doi.org/10.1093/cercor/1.1.1-a

Flood, N.B. (1975) Effect of forebrain ablation on long-term retention of an appetitive discrimination by goldfish. Psychological Reports 36: 783-786. https://doi.org/10.2466/pr0.1975.36.3.783

Folgueira, M., Riva-Mendoza, S., Ferreño-Galmán, N., Castro, A., Bianco, I.H., Anadón, R. & Yáñez. J. (2020) Anatomy and connectivity of the torus longitudinalis of the adult zebrafish. Frontiers in Neural Circuits 14:8. https://doi.org/10.3389/fncir.2020.00008

Folgueira, M., Sueiro, C., Rodríguez-Moldes, I., Yáñez, J., & Anadon, R. (2007). Organization of the torus longitudinalis in the rainbow trout (*Oncorhynchus mykiss):* An immunohistochemical study of the GABAergic system and a DiI tract-tracing study. The Journal of Comparative Neurology, 503: 348–370. https://doi.org/10.1002/cne.21363

Friedlander, M.J. (1983). The visual prosencephalon of teleosts. In: Fish neurobiology. 2. Higher brain areas and functions (R.E. Davis and R.G. Northcutt, eds.). University of Michigan Press, Ann Arbor, pp. 91–115.

Gabriel, J.P., Trivedi, C.A., Maurer, C.M., Ryu, S. and Bollmann, J.H. (2012). Layer-specific targeting of direction-selective neurons in the zebrafish optic tectum. Neuron 76: 1147-1160. https://doi.org/10.1016/j.neuron.2012.12.003

Guthrie, DM; Banks, JR (1978). The receptive field structure of visual cells from the optic tectum of the freshwater perch Perca fluviatilis. Brain Res., 141(2), 211-225. https://doi.org/10.1016/0006-8993(78)90193-2

Guthrie, D.M. & Sharma, S.C. (1991). Visual responses of morphologically identified tectal cells in the goldfish. Vision Research 31, 507–524. https://doi.org/10.1016/0042-6989(91)90102-B

Hagio, H., Sato, M., Yamamoto, N. (2018) An ascending visual pathway to the dorsal telencephalon through the optic tectum and nucleus prethalamicus in the yellowfin goby *Acanthogobius flavimanus* (Temminck & Schlegel, 1845). The Journal of Comparative Neurology 526:1733–1746. https://doi.org/10.1002/cne.24444

Helmbrecht, T.O., Dal Maschio, M., Donovan, J.C., Koutsouli, S., Baier, H. (2018). Topography of a visuomotor transformation. *Neuron* 100:1429–1445. https://doi.org/10.1016/j.neuron.2018.10.021, PMID: 30392799

Ito, H. and R. Kishida. 1978. Telencephalic afferent neurons identified by retrograde HRP method in the carp diencephalon. Brain Research 149: 211–215. https://doi.org/10.1016/0006-8993(78)90600-5

Iwai, E., Saito, S. and Tsukuhara, S. (1970) Analysis of central mechanism in visual discrimination learning of goldfish. Tohoku Journal of Experimental Medicine 102: 135-142. https://doi.org/10.1620/tjem.102.135

Kinoshita, M., Ito, E., Urano, A., Ito, H., & Yamamoto, N. (2006) Periventricular efferent neurons in the optic tectum of rainbow trout. The Journal of Comparative Neurology 499: 546-564. https://doi.org/10.1002/cne.21080

Maximova. E.M., Aliper, A.T., Damjanović, I., Zaichikova, A.A. & Maximov, P.V. (2019) On the organization of receptive fields of retinal spot detectors projecting to the fish tectum: Analogies with the local edge detectors in frogs and mammals. The Journal of Comparative Neurology 528: 1423-1435. https://doi.org/10.1002/cne.24824

Mackintosh, J. & Sutherland, N.S. (1963) Visual discrimination by the goldfish: the orientation of rectangles. Animal Behaviour 11: 135-141. https://doi.org/10.1016/0003-3472(63)90021-6

McClelland, J.L. & Rumelhart, D.E. (1988) Explorations in parallel distributed processing: A handbook of models, programs, and exercises. MIT Press. Cambridge, MA. https://doi.org/10.3758/BF03203842

Meek, J. & Schellart, N.A.M. (1978). A Golgi study of goldfish optic tectum. The Journal of Comparative Neurology 182: 89-122. https://doi.org/10.1002/cne.901820107

Mély, D.A. & Serre, T. (2017) Towards a theory of computation in the visual cortex. In *Computational and Cognitive Neuroscience of Vision*, Q. Zhao ed. Cognitive Science and Technology, Pp 59-84. https://doi.org10.1007/978-981-10-0213-7_4

Meyer, R. L. (1980). Mapping the normal and regenerating projection of goldfish with autoradiographic methods. The Journal of Comparative Neurology 189: 273-289. https://doi.org/10.1002/cne.901890205

Niida, A., Ohno, T. & Iwata, K. S. (1989). Efferent tectal cells of the crucian carp. Physiology and morphology. Brain Research Bulletin 22: 389-398.

Nikolaou, N., Lowe, A.S., Walker, A.S., Abbas, F., Hunter, P.R., Thompson, I.D., and Meyer, M.P. (2012). Parametric functional maps of visual inputs to the tectum. Neuron 76: 317–324. https://doi.org/10.1016/j.neuron.2012.08.040

Nilo, D.A.G., Riegler, C., Hübener, M., & Engert, F. (2021). Distributed chromatic processing at the interface between retina and brain in the larval zebrafish. Current Biology 31: 1945–1953. https://doi.org/10.1016/j.cub.2021.01.088

Northmore, D.P.M. (1977). Spatial summation and light adaptation in the goldfish visual system. Nature 268:450-451. https://doi.org/10.1038/268450a0

Northmore D. P. M. (1984). Visual and saccadic activity in the goldfish torus longitudinalis. Journal of Comparative Physiology A. 155: 333-340. https://doi.org/10.1007/BF00610587

Northmore, D.P.M. (2017). Holding visual attention for 400 million years: A model of tectum and torus longitudinalis in teleost fishes. Vision Research 131: 44–56. https://doi.org/10.1016/j.visres.2016.12.001

Northmore, D.P.M. (2023). In the beginning there was dimming: OFF pathways from retina through optic tectum to torus longitudinalis in fish. ResearchGate preprint. https://doi.org/10.13140/RG.2.2.26188.08328

Northmore, D.P.M. & Dvorak, C.A. (1979) Contrast sensitivity and acuity of the goldfish. Vision Research 19: 255-261. https://doi.org/10.1016/0042-6989(79)90171-8

Northmore, D.P.M. & Oh, D.-J. (1998) Axonal conduction velocities of functionally characterized retinal ganglion cells in goldfish. Journal of Physiology 506: 207-217. https://doi.org/10.1111/j.1469-7793.1998.207bx.x

Northmore, D.P.M. & Sharma, S.C. (1979) Visual sensitivity and spatial summation in goldfish with compressed retinotectal projections or total tectal ablation. Brain Research 180: 344-348. https://doi.org/10.1016/0006-8993(79)90340-8

Northmore D. P. M., Williams B. & Vanegas H. (1983). The teleostean torus longitudinalis: responses related to eye movements, visuotopic mapping, and functional relations with the optic tectum. Journal of Comparative Physiology A. 150: 39-50. https://doi.org/10.1007/BF00605286

O'Benar, J.D. (1976) Electrophysiology of neural units in goldfish optic tectum. Brain Research Bulletin 1:529-541. https://doi.org/10.1016/0361-9230(76)90080-0

Ohnishi, K. (1991). Goldfish visual information-processing patterns in food-reinforced discrimination-learning between compound visual-stimuli. Journal of Comparative Physiology A 168: 581-589. https://doi.org/10.1007/BF00215080

Parker, A.N., Wallis, G.M., Obergrussberger, R. , & Siebeck, U.E. (2020) Categorical face perception in fish: How a fish brain warps reality to dissociate "same" from "different". Journal of Comparative Neurology 528: 2919– 2928. https://doi.org/10.1002/cne.24947

Preuss, S.J., Trivedi, C.A., vom Berg-Maurer, C.M., Ryu, S., Bollmann, J.H. (2014) Classification of object size in retinotectal microcircuits. Current Biology 24: 2376-2385. https://doi.org/10.1016/j.cub.2014.09.012

Reichenthal, A., Segev, R. & Ben-Shahar, O., (2020) Feature integration theory in non-humans: spotlight on the archerfish. Attention, Perception, & Psychophysics 82:752–774. https://doi.org/10.3758/s13414-019-01884-4

Robles, E., Filosa, A. and Baier, H. (2013) Precise Lamination of Retinal Axons Generates Multiple Parallel Input Pathways in the Tectum. The Journal of Neuroscience 33:5027–5039. https://doi.org/10.1523/JNEUROSCI.4990-12.2013

Robles, E., Fields, N.P., & Baier, H. (2021). The zebrafish visual system transmits dimming information via multiple segregated pathways. The Journal of Comparative Neurology 529: 539-552. https://doi.org/10.1002/cne.24964

Robles, E., Laurell, E. & Baier, H. (2014). The retinal projectome reveals brain-area-specific visual representations generated by ganglion cell diversity. Current Biology 24: 2085–2096. http://dx.doi.org/10.1016/j.cub.2014.07.080

Rowe, J.S. & Beauchamp, R.D. (1982). Visual responses of nucleus corticalis neurons in the perciform teleost, Northern Rock Bass (*Ambloplites rupestris rupestris).* Brain Research 236: 205-209. https://doi.org/10.1016/0006-8993(82)90047-6

Rumelhart, D.E. & McClelland, J.L. (1986). On learning the past tenses of English verbs. In *Parallel Distributed Processing: Explorations in the Microstructure of Cognition,* Volume 2, Pp 216–271. MIT Press, Cambridge, MA.

Saidel, W.M., Marquez-Houston, K. & Butler, A.B. (2001). Identification of visual pallial telencephalon in the goldfish, *Carassius auratus*: a combined cytochrome oxidase and electrophysiological study. Brain Research 919: 82-93. https://doi.org/10.1016/S0006-8993(01)03001-3

Sajovic, P., & Levinthal, C. (1982). Visual response properties of zebrafish tectal cells. Neuroscience 7: 2427–2440. https://doi.org/10.1016/0306-4522(82)90205-6

Serre, T. (2014). Hierarchical models of the visual system. Encyclopedia of Computational Neuroscience 6: 1-12.

Sovrano, V.A. & Bisazza, A. (2009) Perception of subjective contours in fish. Perception:38, 579 – 59. https://doi.org/10.1068/p6121

Schellart, N.A.M. & Spekreijse, H. (1976). Shapes of receptive field centers on optic tectum of goldfish. Vision Research 16: 1018–1020. https://doi.org/10.1016/0042-6989(76)90236-4

Schwassmann, H.O. & Kruger, L. (1965). Organization of the visual projection upon the optic tectum of some freshwater fish. The Journal of Comparative Neurology 124: 113-126. https://doi.org/10.1002/cne.901240109

Sutherland, N.S. (1968). Outlines of a theory of visual pattern recognition in animals and man. Proceedings of the Royal Society of London. B. 171: 297-317. https://doi.org/10.1098/rspb.1968.0072

Sutherland, N.S. & Bowman, R. (1969) Discrimination of circles and squares with and without knobs by goldfish, Quarterly Journal of Experimental Psychology, 21: 330-338. https://doi.org/10.1080/14640746908400228

Treisman, A. M., & Gelade, G. (1980). A feature-integration theory of attention. Cognitive Psychology, 12: 97-136. https://doi.org/10.1016/0010-0285(80)90005-5

Vanegas, H., Williams, B., & Freeman, J. A. (1979). Responses to stimulation of marginal fibers in the teleostean optic tectum. Experimental Brain Research, 34: 335–349. https://doi.org/10.1007/BF00235677

Wang, K. Hinz, J., Zhang, Y., Thiele, T.R., & Arrenberg, A.B. (2020). Parallel channels for motion feature extraction in the pretectum and tectum of larval zebrafish. Cell Reports 30: 442–453. https://doi.org/10.1016/j.celrep.2019.12.031

Wullimann, M. F. (1994). The teleostean torus longitudinalis: A short review on its structure, histochemistry, connectivity, possible function and phylogeny. European Journal of Morphology, 32, 235–242.

Wyzisk, K. & Neumeyer, C. (2007). Perception of illusory surfaces and contours in goldfish. Visual Neuroscience 24: 291-298. https://doi.org/10.1017/S095252380707023X

Xue, H.-G., Yamamoto, N., Yang, C.-Y., Kerem, G., Yoshimoto, M., Imura, K., & Ito, H. (2003). Fiber connections of the torus longitudinalis and optic tectum in Holocentrid teleosts. The Journal of Comparative Neurology, 462: 194–212. https://doi.org/10.1002/cne.10730

Yager, D., Sharma, S.C., & Grover, B.G. (1977). Visual function in goldfish with unilateral and bilateral tectal ablation, Brain Research, 137: 267-275. https://doi.org/10.1016/0006-8993(77)90338-9.

Yamamoto, N. & Hagio, H. (2021). Cerebellum-like systems in actinopterygian fishes with a special focus on the diversity of cerebellum-like system in the mesencephalon. Ch. 2 in *Cerebellum as a CNS Hub.* H. Mizusawa, S. Kakei (eds.), Contemporary Clinical Neuroscience, Springer Nature, Switzerland. https://doi.org/10.1007/978-3-030-75817-2_2

Yañez, J., Suárez, T., Quelle, A., & Folgueira., M. (2018) Neural connections of the pretectum in zebrafish (*Danio rerio).* The Journal of Comparative Neurology 526:1017-1040. https://doi.org/10.1002/cne.24388

Zhaoping, L. (2016) From the optic tectum to the primary visual cortex: migration through evolution of the saliency map for exogenous attentional guidance. Current Opinion in Neurobiology 40:94–102.
https://doi.org/10.1016/j.conb.2016.06.017